Elemental chalcogens as a minimal model for charge and orbital order

Silva, A.; Henke, J.; van Wezel, J.

DOI
10.1103/PhysRevB.97.045151
Publication date
2018
Document Version
Final published version
Published in
Physical Review B

Elemental chalcogens as a minimal model for combined charge and orbital order

Ana Silva, Jans Henke, and Jasper van Wezel
Institute for Theoretical Physics, Institute of Physics, University of Amsterdam, 1090 GL Amsterdam, The Netherlands

(Received 16 June 2017; revised manuscript received 16 October 2017; published 30 January 2018)

Helices of increased electron density emerging spontaneously in materials containing multiple, interacting density waves, are an example of how orbital and charge degrees of freedom may combine to form a single ordered phase. Although a macroscopic order parameter theory describing this behavior has been proposed and experimentally tested, a microscopic understanding of such simultaneous orbital and electronic order in specific materials is still lacking. Here we present the elemental chalcogens selenium and tellurium as model materials for the development of combined charge and orbital order. We formulate minimal models capturing the formation of spiral structures consisting of ordered occupied orbitals and increased charge density, both in terms of a macroscopic Landau theory and a microscopic Hamiltonian. Both reproduce the known chiral crystal structure and are consistent with its observed thermal evolution and behavior under pressure. The combination of microscopic and macroscopic frameworks allows us to distill the essential ingredients in the emergence of combined orbital and charge order, and may serve as a general guide to predicting and understanding spontaneous chirality as well as other, more general, types of combined charge and orbital order in other materials.

DOI: 10.1103/PhysRevB.97.045151

I. INTRODUCTION

The bulk transition metal dichalcogenide *1T*-$TiSe_2$ has been shown, uniquely, to harbor a charge density wave transition that breaks inversion symmetry in a chiral way [1–5]. In contrast to the well-known chirality of spins in helical magnets, the formation of spirals within the scalar electronic density cannot occur by itself, and is necessarily accompanied by the onset of simultaneous orbital order [3,6,7]. The result is an example of a novel type of order, in which the orbital and charge degrees of freedom are combined into a single order parameter. Similar chiral order has been theoretically suggested to determine material properties of various transition metal dichalcogenides [8–10], and even cuprate high-temperature superconductors [11–13]. But the cooperation between charge and orbital degrees of freedom is not restricted to chiral phases. The two degrees of freedom have, for example, also already been proposed to combine into a polar order parameter [10], and there is no reason to believe this exhausts the list of possible novel phases.

Focusing first on the chiral combination of charge and orbitals, indirect evidence for the presence of spiral charge order was found in scanning-tunneling microscopy experiments on *1T*-$TiSe_2$ [1,5]. In addition, several predictions arising from a Ginzburg-Landau theory of the chiral phase transition were experimentally confirmed [3–5]. Nevertheless, it has proven difficult to obtain direct experimental confirmation of the broken inversion symmetry. The main reason for this is believed to be the presence of small, nanometer wide, domains of varying handedness [5], averaged over by almost all direct bulk probes. A microscopic understanding, going beyond the predictions of the macroscopic order parameter theory, is thus essential in the search for further experiments able to directly probe this novel type of combined charge and orbital order.

A microscopic theory for the chiral state of *1T*-$TiSe_2$ would necessarily involve all 22 orbitals in its unit cell. Even if such a model were constructed, its inherent complexity would obscure a general understanding of how charge and orbital degrees of freedom cooperate to form a single ordered phase, and would likely not be useful as a guide to identifying other possible materials that can harbor electronic spirals or other types of combined charge and orbital order. We therefore take an alternative approach, and formulate a minimal microscopic model for the appearance of spiral chains in the atomic structure of the elemental chalcogens Se and Te, which we propose to be prototype materials for combined orbital and charge order in general. These materials are well known to have a chiral crystal structure at ambient conditions. The handedness of a given sample is evidenced by both its diffraction pattern and optical activity [14]. The crystal structure can be viewed as short bonds arranged along helices in a simple cubic lattice, as shown schematically in Fig. 1(a) [14]. Although Se and Te do not exhibit a charge ordering transition at any temperature, the spiral bond order is understood as an instability of a simple cubic parent lattice structure [2,6,7]. The charge ordering transition from the hypothetic simple cubic to the actual chiral phase is known to be of the same type as the chiral transition in *1T*-$TiSe_2$ [3]. Owing to the simple lattice structure however, an explicit and easily accessible microscopic model can be formulated for Te and Se, elucidating how different types of electron-phonon coupling and Coulomb interactions conspire to form the spiral structure. This model is presented here as a minimal description for combined charge and orbital order in general.

II. INTUITIVE PICTURE

Before presenting both macroscopic and microscopic models of the chiral charge order, we first give an intuitive picture showcasing their basic ingredients. The starting point is the simple cubic lattice structure. Both Se and Te crystals possess the chiral structure shown in Fig. 1(a) for any temperature at ambient pressure. Upon melting Te however, the short-ranged

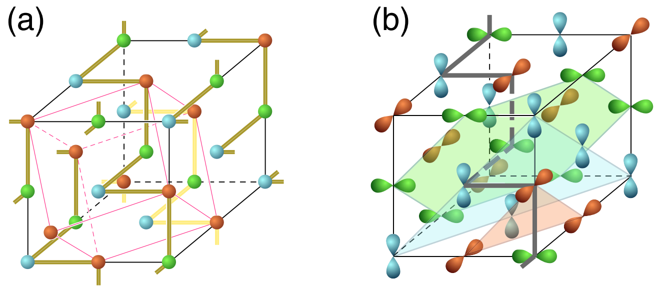

FIG. 1. (a) The chiral crystal structure of Se and Te can be understood as a spiral arrangement of short bonds in a simple cubic parent lattice. Atoms with different colors indicate the three possible local configurations of short bonds. The chiral unit cell is indicated in pink. (b) The short bonds involve charge transfer between specific orbitals only, causing the chiral crystal lattice to also be orbital ordered. Note that since the electronic system is 2/3 filled, the orbital order shown consists of the least occupied orbitals. The shaded planes, included as a guide to the eye, connect like orbitals and are perpendicular to the spiral axis.

chiral order in the fluid turns into a more cubic, metallic phase at a crossover temperature not much above the melting point [15–17]. This observation can be understood as a latent structural phase transition, which is preempted by the material melting before the transition temperature can be reached. In fact, in the element Po, which is isoelectronic to Se and Te and sits just below them in the periodic table, strong spin-orbit coupling prevents the formation of chiral order and allows the underlying simple cubic lattice structure to remain visible even at low temperatures [18,19].

Within a simple cubic lattice, the four valence electrons (2/3 filling) of elemental chalcogens are distributed among p orbitals that may be chosen to point along the crystallographic x, y, and z axes. The overlap between neighboring p_x orbitals on the x axis is significantly larger than that between neighboring p_x orbitals on the y or z axes, or between p orbitals of different type. Taking this difference to the extreme limit, we consider a minimal model in which only overlaps between orbitals aligned in a head-to-toe manner are nonzero. Although quantitatively unrealistic, it captures all qualitative aspects of the chiral phase transition.

In that limit, an electron in for example a p_x orbital can only hop in the x direction, onto a neighboring p_x orbital. The simple cubic lattice is thus filled with interwoven but independent one-dimensional chains running in all three lattice directions. The electronic structure consists of three one-dimensional bands, each producing a pair of parallel planar Fermi surfaces in the first Brillouin zone. The Fermi surface is extremely well nested, and a Peierls-type charge density wave is expected to emerge [20]. In fact, a single nesting vector $\mathbf{Q}$, corresponding to a body diagonal of the cube of intersecting Fermi surfaces, connects each point on any of the Fermi surface sheets to a point within a parallel sheet. The dominant instability will therefore be towards the formation of charge density waves $\rho_j(\mathbf{x}) = \rho_0 + A\cos(\mathbf{Q}\cdot\mathbf{x})$ in each of the three orbital sectors (labeled by j), who all share the same propagation direction $\mathbf{Q}$. Here ρ_0 is the average charge density in the normal state, and A is the amplitude of the charge modulation.

The atomic displacement waves $\mathbf{u}_j(\mathbf{x}) = \tilde{u}\mathbf{e}_j\sin(\mathbf{Q}\cdot\mathbf{x})$, forming in response to the charge modulations, have polarizations $\mathbf{e}_j$ whose direction is determined by the anisotropy of the local electron-phonon coupling matrix elements [3]. In a chain of p_x orbitals with overlaps only along x, the electron-phonon coupling is maximally anisotropic, and the displacement direction $\mathbf{e}$ will be purely along x. The three orthogonal chains running through each atom act independently, and the actual atomic displacement is the sum of the three contributions $\mathbf{u}_j$.

The charge density wave in each orbital chain can be shifted along its propagation direction by the addition of a phase: $\rho_j(\mathbf{x}) \propto \cos(\mathbf{Q}\cdot\mathbf{x} + \varphi_j)$. A Coulomb interaction between charges in orthogonal orbitals on the same site, will cause the charge maxima along one chain to prefer to avoid those of other chains, effectively coupling the phases in different orbital sectors. The lowest energy configuration then produces precisely the charge redistribution and lattice deformations shown in Fig. 1(a), which agree with the experimentally observed crystal structure of Se and Te [2,6]. Each atom in this final structure has a single least occupied p orbital. The chiral charge ordered structure is therefore also automatically an orbital ordered phase, as shown in Fig. 1(b).

III. MACROSCOPIC ORDER PARAMETER THEORY

A Landau free energy may be written in terms of the dimensionless order parameters $\alpha_j(\mathbf{x})$ representing the periodic modulation of the charge density within a given chain of head-to-toe orbitals: $\rho_j(\mathbf{x}) = \rho_0[1 + \alpha_j(\mathbf{x})]$. If the orbital sectors are noninteracting, their free energies are independent: $F_j = \int d^3x\ a(\mathbf{x})\alpha_j^2 + b(\mathbf{x})\alpha_j^3 + c(\mathbf{x})\alpha_j^4$. Notice that the presence of the lattice is taken into account by expanding the coefficients in terms of reciprocal lattice vectors, so that for example $a(\mathbf{x}) = a_0 + a_1\sum_n e^{i\mathbf{G}_n\cdot\mathbf{x}} + \cdots$ [21]. Here $\mathbf{G}_n$ denote the shortest reciprocal lattice vectors. Terms a_j with $j > 0$ in this sum arise from the electron-phonon coupling in a more microscopic model.

The on-site Coulomb interaction provides the interaction terms $F_{\rm Coul} = \sum_j \int d^3x\ A_0\alpha_j\alpha_{j+1}$. The periodic charge distributions can be written as $\alpha_j(\mathbf{x}) = \psi_0\cos(\mathbf{Q}\cdot\mathbf{x} + \varphi_j)$, with the amplitude ψ_0 equal for all three order parameters, and φ_j is a spatial shift of the charge density wave along j. Performing the integration over $\mathbf{x}$, the full free energy, per volume, becomes

$$F = \frac{3}{2}a_0\psi_0^2 + \frac{9}{8}c_0\psi_0^4 + \frac{1}{4}b_1\psi_0^3\sum_j\cos(3\varphi_j) + \frac{1}{2}A_0\psi_0^2\sum_j\cos(\varphi_j - \varphi_{j+1}). \tag{1}$$

As usual, the temperature dependence is considered by expanding a_0 as a function of $T - T_c$, near the critical temperature. In this way, a_0 determines when the free energy has a minimum at nonzero values of ψ_0, and charge order sets in. The final two terms, arising from the electron-phonon coupling and the Coulomb interaction, respectively, determine the values of the phases φ_j. They can be simultaneously minimized by taking $\varphi_1 = n\pi/3$, where n is an odd or even integer depending on the sign of b_1. Physically, this corresponds to the charge order being either site or bond centered. Additionally, the relative phase differences should be chosen as $\varphi_j - \varphi_{j+1} = \pm 2\pi/3$. These solutions are then precisely the left- and right-handed chiral configurations, one of which is shown in Fig. 1(a).

Comparing the free energy of Eq. (1) to the one given for $1T$-$TiSe_2$ in Ref. [3], it appears that in spite of the different underlying atomic and electronic configurations, the routes to chiral charge and orbital order are largely the same. The onset of charge order from a disordered state is determined by amplitude terms only. Electron-phonon coupling then favors locking of the different charge density wave contributions to the lattice. The on-site Coulomb interaction finally couples density waves in distinct orbital sectors, leading to relative phase shifts and the emergence of chiral charge and orbital order.

Upon applying uniform pressure, Se and Te undergo a series of structural transitions into nonchiral phases [22,23]. This can be understood within the free energy expansion as a pressure dependence of the critical temperature, which we write as $a_0(T,P) = \frac{3b_1^2}{32c_0} + \frac{A_0}{2} + \alpha[\frac{T}{T_C^0} + \frac{P}{P_C^0} - 1]$. Here P_C^0 is the critical pressure at zero temperature, while T_C^0 is the critical temperature at zero applied pressure. The constant term in a_0 is needed to guarantee that, after minimizing F with respect to the phase variables, the total prefactor of ψ_0^2 becomes negative, and a nonzero ψ_0 develops, when T decreases below $T_C^0(1 - P/P_C^0)$. Notice that the relation between critical temperature and pressure is thus assumed to be linear, and that the high-pressure, nonchiral phase is assumed to always be simple cubic. In spite of these simplifications, the free energy expansion captures the suppression of combined charge and orbital order by pressure, and may be straightforwardly extended to describe uniaxial as well as uniform pressure.

The amplitudes ψ_j in different orbital sectors may be allowed to each have their own critical temperature, depending on the amount of pressure applied along a particular axis. The free energy then becomes

$$F = \sum_j \frac{1}{2}a_0(T,P_j)\psi_j^2 + \frac{3}{8}c_0\psi_j^4 + \frac{1}{4}b_1\psi_j^3\cos(3\varphi_j) + \frac{1}{2}A_0\psi_j\psi_{j+1}\cos(\varphi_j - \varphi_{j+1}). \quad (2)$$

Applying uniaxial pressure suppresses only one of the charge density wave components. As T is now decreased from high temperatures, one of the $a_0(T,P_j)$ terms will remain positive while the others already cause order to set in their associated orbital sectors. There is thus a range of temperatures for which the charge order is confined to two orbital sectors only. This results in stacked planes, each containing zigzag charge order, as indicated in Fig. 2, which also shows the phase diagram resulting from this minimal model. The anisotropic structure agrees both with the predictions of an earlier semiclassical approach in terms of so-called vector charge density waves [6], and with the experimental observation of layered structures in Se under pressure [22,23].

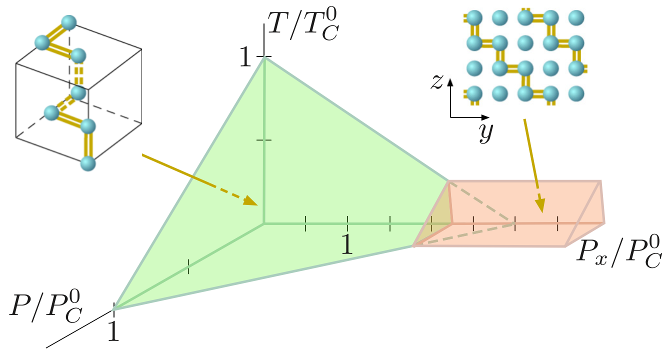

FIG. 2. Schematic phase diagram indicating the relative stability of the chiral and zigzag phases within the free energy of Eq. (2). The zigzag chains occur in planes perpendicular to the strain direction. The applied pressure along the (x, y, z) axes is parametrized as $(P + P_x, P, P)$. Notice that the linearity of the critical lines and planes results from the linear thermal and pressure dependencies assumed in a_0.

IV. MICROSCOPIC MODEL

To see how the terms in the Landau free energy emerge from the interplay of microscopic degrees of freedom, we start again from a 2/3-filled p shell within the simple cubic lattice. Including hopping only between head-to-toe orbitals, the tight-binding Hamiltonian can be written as

$$\hat{H} = \hat{H}_{\rm TB} + \hat{H}_{\rm Coul} + +\hat{H}_{\text{e-ph}} + H_{\rm boson},$$
$$\hat{H}_{\rm TB} = t\sum_{\mathbf{x},j}\hat{c}_j^\dagger(\mathbf{x})\hat{c}_j(\mathbf{x}+\mathbf{a}_j) + \text{H.c.},$$
$$\hat{H}_{\rm Coul} = V\sum_{\mathbf{x},j}\hat{c}_j^\dagger(\mathbf{x})\hat{c}_j(\mathbf{x})\hat{c}_{j+1}^\dagger(\mathbf{x})\hat{c}_{j+1}(\mathbf{x}),$$
$$\hat{H}_{\rm boson} = \hbar\omega\sum_{\mathbf{q},j}\hat{b}_j^\dagger(\mathbf{q})\hat{b}_j(\mathbf{q}).$$

Here $\hat{c}_j^\dagger(\mathbf{x})$ creates an electron in orbital j on position $\mathbf{x}$, and $\mathbf{a}_j$ is the simple cubic lattice vector in direction j. The hopping amplitude t is positive, since overlapping orbital lobes on neighboring sites have opposite signs. The Coulomb interaction acts on-site only, and the displacement $\hat{u}_j(\mathbf{x})$ of the atom on position $\mathbf{x}$ in the direction of j is written in terms of the phonon operator $\hat{b}_j^\dagger(\mathbf{x})$, taken to be a dispersionless Einstein mode. The electron-phonon coupling $\hat{H}_{\text{e-ph}}$ consists of two contributions:

$$\hat{H}_{\text{e-ph}}^{(1)} = \alpha^{(1)}\sum_{\mathbf{x},j}(\hat{u}_j(\mathbf{x}) - \hat{u}_j(\mathbf{x}+\mathbf{a}_j)) \times (\hat{c}_j^\dagger(\mathbf{x})\hat{c}_j(\mathbf{x}+\mathbf{a}_j) + \hat{c}_j^\dagger(\mathbf{x}+\mathbf{a}_j)\hat{c}_j(\mathbf{x})),$$
$$\hat{H}_{\text{e-ph}}^{(2)} = \alpha^{(2)}\sum_{\mathbf{x},j}(\hat{u}_j(\mathbf{x}+\mathbf{a}_j) - \hat{u}_j(\mathbf{x}-\mathbf{a}_j))\hat{c}_j^\dagger(\mathbf{x})\hat{c}_j(\mathbf{x}).$$

The first type of electron-phonon coupling affects the kinetic energy of electrons, by increasing the hopping amplitude if the interatomic distance decreases. The second process lowers the electronic potential energy in regions of increased ionic density.

The full Hamiltonian can be diagonalized in the mean field approximation, using ansatz averages that reflect the ordered states found in the Landau theory analysis:

$$\langle\hat{c}_j^\dagger(\mathbf{x})\hat{c}_j(\mathbf{x})\rangle = \rho_0 + A\cos(\mathbf{Q}\cdot\mathbf{x} + \varphi_j),$$
$$\langle\hat{c}_j^\dagger(\mathbf{x})\hat{c}_j(\mathbf{x}+\mathbf{a}_j)\rangle = \sigma_0 + B\cos[\mathbf{Q}\cdot(\mathbf{x}+\mathbf{a}_j)/2 + \chi_j],$$
$$\langle\hat{u}_j(\mathbf{x})\rangle = \tilde{u}\sin(\mathbf{Q}\cdot\mathbf{x} + \phi_j).$$

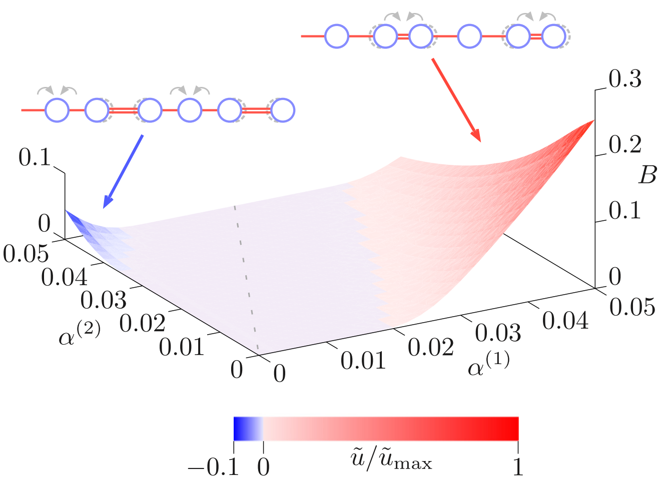

FIG. 3. The ground state phase diagram as a function of the two contributions to the electron-phonon coupling. The vertical axis shows the order parameter B, while the colors indicate the normalized atomic displacement. Two possible types of chiral charge and orbital ordered state are shown schematically in the insets. Increased bond density is indicated by double lines, while curved arrows indicate charge transfer from or onto atomic sites.

Here A is the mean field for modulations of the on-site charge density, B is for the bond density, and $\tilde{u}$ is for the atomic positions. Course graining of the mean fields A and B would yield the Landau order parameter α, while the values of coefficients appearing in the Landau theory can in principle be obtained from the microscopic model by calculating loop diagrams [24].

The bosonic part of the mean field Hamiltonian can be diagonalized by introducing a new set of operators defined as $\hat{\gamma}_j(\mathbf{q}) = \hat{b}_j(\mathbf{q}) + v_{\mathbf{q},j}\delta(\mathbf{q}-\mathbf{Q}) + w_{\mathbf{q},j}\delta(\mathbf{q}+\mathbf{Q})$ [25]. Requiring this transformation to bring the bosonic Hamiltonian into diagonal form determines the values of $v_{\mathbf{q},j}$ and $w_{\mathbf{q},j}$. The expectation values of the of the displacement operators $\hat{u}_j$ can then be computed in the diagonal basis, which yields the relation between atomic displacements and the electronic order parameters: $\tilde{u} = 2\sqrt{3}/\hbar\omega(2B\alpha^{(1)}e^{(\chi_j-\phi_j)} - A\alpha^{(2)}e^{i(\varphi_j-\phi_j)})$. Demanding the displacement to be real restricts the phase differences to be integer multiples of π.

The fermionic part of the Hamiltonian can be diagonalized numerically. The values of the order parameter phases and amplitudes are determined self-consistently, by requiring that the expectation values computed using particular ansatz averages match the ansatz values. With zero on-site Coulomb interaction, the orbital sectors independently develop charge density waves. The phases are $\varphi_j = n_j\pi/3$, with n_j integer, which includes both nonchiral solutions in which the n_j are all equal, and chiral ones. For any nonzero value of the Coulomb interaction, this degeneracy is lifted, and the left- and right-handed chiral charge ordered configurations with $n_j - n_{j+1} = \pm 2\pi/3$ become the lowest energy states.

For each handedness, the n_j may be odd or even multiples of $\pi/3$. These solutions correspond to either bond-centered or site-centered charge density waves, as indicated in the insets of Fig. 3. The bond-centered solution dominates for large $\alpha^{(1)}/\alpha^{(2)}$, while the site-centered one is consistent with the opposite regime. The atomic structure observed in elemental Se and Te corresponds to the bond-centered charge order [14], with $\alpha^{(1)}$ prevailing.

Within the chiral phase, the short bonds in the three orbital chain directions connect to form a spiral, in agreement with the experimentally observed structure shown schematically in Fig. 1(a). The displacements in the x, y, and z directions arise from charge order in chains of p_x, p_y, and p_z orbitals, respectively. The modulation of charge density can thus also be seen as a spatial modulation of orbital occupation, as shown explicitly in Fig. 1(b). The emergence of orbital order in conjunction with chiral charge order is inevitable, since both arise from the same relative phase shifts between charge density waves in distinct orbital sectors. The presence of an interaction between charge density wave components leading to relative phase shifts, can thus be interpreted as a generic route to combined charge and orbital order, which should be applicable to a wide range of materials hosting multicomponent charge order.

V. DISCUSSION

Although a phase of combined charge and orbital order has been proposed to exist in the low-temperature phase of *1T*-$TiSe_2$ [1,3,4], the broken inversion symmetry is yet to be observed directly. In addition, the interplay between the great number of atoms within the unit cell of $TiSe_2$ complicate the extraction of physical insight from microscopic models [26,27]. Having a model material, which harbors a similar charge and orbital ordered state but is structurally simple and well understood, is therefore crucial to aid in building a general understanding of this novel state of matter, and in allowing the identification of related novel types of order in other materials. We argue that the elemental chalcogens tellurium and selenium constitute precisely such model materials.

In both the elemental chalcogens and *1T*-$TiSe_2$ multiple density wave instabilities occur in distinct orbital sectors. These give rise to multiple, differently polarized, displacement waves in both materials. The on-site Coulomb repulsion then causes maxima of different density waves to repel each other. This results in shifting of the density waves, thus breaking inversion symmetry and yielding a chiral crystal structure (as long as no mirror symmetries in the parent lattice reduce the chiral order to polar [8–10]). The density waves originating in distinct orbital sectors, necessarily implies that orbital order accompanies the charge modulations, creating a combined charge and orbital ordered phase.

In contrast to the chalcogens, the propagation vectors for different density waves in $TiSe_2$ are all distinct. The order is also site centered in Se and Te, but bond centered in $TiSe_2$. Finally, the on-site Coulomb repulsion coupling different density waves, yields only an indirect interaction between bond-centered charges in the case of $TiSe_2$. Despite these and other differences, including for example the different driving mechanisms underlying the density wave formation [25,28], a common general mechanism for combining charge and orbital order is identified: as long as multiple density wave instabilities occur in distinct sections of the Fermi surface, which correspond to distinct orbital textures, any local interaction between orbital sections will cause the combination of charge and orbital order into a single ordered phase. We thus predict that a type of combined order can be found in any charge ordered material involving multiple orbital sectors, including (families of) materials with much more complicated structures than the elemental chalcogens. The theoretical understanding developed here for Se and Te can be used as a guiding principle in looking for such novel states of matter.

ACKNOWLEDGMENTS

J.v.W. acknowledges support from VIDI Grant No. 680-47-528, financed by the Netherlands Organisation for Scientific Research (NWO).

[1] J. Ishioka, Y. H. Liu, K. Shimatake, T. Kurosawa, K. Ichimura, Y. Toda, M. Oda, and S. Tanda, Phys. Rev. Lett. **105**, 176401 (2010).
[2] J. van Wezel and P. Littlewood, Physics **3**, 87 (2010).
[3] J. van Wezel, Europhys. Lett. **96**, 67011 (2011).
[4] J.-P. Castellan, S. Rosenkranz, R. Osborn, Q. Li, K. E. Gray, X. Luo, U. Welp, G. Karapetrov, J. P. C. Ruff, and J. van Wezel, Phys. Rev. Lett. **110**, 196404 (2013).
[5] M. Iavarone, R. Di Capua, X. Zhang, M. Golalikhani, S. A. Moore, and G. Karapetrov, Phys. Rev. B **85**, 155103 (2012).
[6] H. Fukutome, Prog. Theor. Phys. **71**, 1 (1984).
[7] Y. Shimoi and H. Fukutome, Prog. Theor. Phys. **87**, 307 (1992).
[8] J. van Wezel, Physica B **407**, 1779 (2012).
[9] I. Guillamón, H. Suderow, J. G. Rodrigo, S. Vieira, P. Rodière, L. Cario, E. Navarro-Moratalla, C. Martí-Gastaldo, and E. Coronado, New J. Phys. **13**, 103020 (2011).
[10] J. van Wezel, Phys. Rev. B **85**, 035131 (2012).
[11] P. Hosur, A. Kapitulnik, S. A. Kivelson, J. Orenstein, and S. Raghu, Phys. Rev. B **87**, 115116 (2013).
[12] P. Hosur, A. Kapitulnik, S. A. Kivelson, J. Orenstein, S. Raghu, W. Cho, and A. Fried, Phys. Rev. B **91**, 039908(E) (2015).
[13] M. Gradhand and J. van Wezel, Phys. Rev. B **92**, 041111(R) (2015).
[14] Y. Tanaka, S. P. Collins, S. W. Lovesey, M. Matsumami, T. Moriwaki, and S. Shin, J. Phys. Condons. Matter **22**, 122201 (2010).
[15] R. Bellissent and G. Tourand, J. Non-Cryst. Solid **35**, 1221 (1980).
[16] M. Inui, T. Noda, and K. Tamura, J. Non-Cryst. Solid **205**, 261 (1996).
[17] G. Tourand, Phys. Lett. A **54**, 209 (1975).
[18] W. H. Beamer and C. R. Maxwell, J. Chem. Phys. **14**, 569 (1946).
[19] C.-J. Kang, K. Kim, and B. I. Min, Phys. Rev. B **86**, 054115 (2012).
[20] R. E. Peierls, *More Surprises in Theoretical Physics* (Princeton University Press, Princeton, NJ, 1991).
[21] W. L. McMillan, Phys. Rev. B **14**, 1496 (1976).
[22] Y. Akahama, M. Kobayashi, and H. Kawamura, Phys. Rev. B **47**, 20 (1993).
[23] O. Degtyareva, E. Gregoryanz, H. K. Mao, and R. J. Hemley, High Press. Res. **25**, 17 (2005).
[24] F. Flicker, and J. van Wezel, Nat. Commun. **6**, 7034 (2015).
[25] J. van Wezel, P. Nahai-Williamson, and S. S. Saxena, Phys. Rev. B **81**, 165109 (2010).
[26] B. Zenker, H. Fehske, H. Beck, C. Monney, and A. R. Bishop, Phys. Rev. B **88**, 075138 (2013).
[27] S. Zhu and J. van Wezel (to be published).
[28] A. Kogar, M. S. Rak, S. Vig, A. A. Husain, F. Flicker, Y. I. Joe, L. Venema, G. J. MacDougall, T. C. Chiang, E. Fradkin, J. van Wezel, and P. Abbamonte, Science **358**, 1314 (2017).